

## 基于双席夫碱配体的两个锰(III)配合物的合成、 晶体结构和抑制脲酶活性

李运彤<sup>1</sup> 董靖雯<sup>1</sup> 芦 瑶<sup>2</sup> 谷易桐<sup>1</sup> 商超男<sup>1</sup>

刘芙瑶<sup>1</sup> 辛 雨<sup>1</sup> 井长玲<sup>1</sup> 由忠录<sup>\*1</sup>

(<sup>1</sup> 辽宁师范大学化学化工学院, 大连 116029)

(<sup>2</sup> 辽西育明高级中学, 锦州 121000)

**摘要:** 制备了一个双席夫碱 *N,N'*-双(3,5-二氟亚水杨基)-1,3-二氨基丙烷( $H_2L$ )。利用  $H_2L$ 、醋酸锰和硫氰酸铵或者叠氮化钠在甲醇中反应分别制得了配合物  $[MnL(NCS)(OH_2)]$  (**1**)和  $[MnL(\mu_{1,3}-N_3)]_n$  (**2**)。通过元素分析、红外光谱、核磁共振氢谱对  $H_2L$  和其配合物进行了表征,用单晶 X 射线衍射测定了配合物的结构。席夫碱配体利用其亚胺基氮原子和酚羟基氧原子与 Mn 进行配位。硫氰酸根配体利用其氮原子配位,而叠氮根配体利用两端的氮原子以桥联的方式进行配位。在每个配合物中, Mn 原子都采取八面体配位构型。测试了  $H_2L$  和 2 个配合物对刀豆脲酶的抑制活性。在浓度为  $100 \mu\text{mol}\cdot\text{L}^{-1}$  时,配合物 **1** 对脲酶的抑制率为  $(52.0\pm 3.1)\%$ ,其  $IC_{50}$  值为  $(81.0\pm 3.7) \mu\text{mol}\cdot\text{L}^{-1}$ ,而配合物 **2** 却没有活性。还利用分子对接技术研究了配合物 **1** 与脲酶的作用方式。

**关键词:** 席夫碱; 锰配合物; 晶体结构; 脲酶抑制剂

中图分类号: O614.71<sup>†1</sup>

文献标识码: A

文章编号: 1001-4861(2018)06-1192-07

DOI: 10.11862/CJIC.2018.147

## Syntheses, Crystal Structures and Urease Inhibition of Two Manganese(III) Complexes with Bis-Schiff Bases

LI Yun-Tong<sup>1</sup> DONG Jing-Wen<sup>1</sup> LU Yao<sup>2</sup> GU Yi-Tong<sup>1</sup> SHANG Chao-Nan<sup>1</sup>

LIU Fu-Yao<sup>1</sup> XIN Yu<sup>1</sup> JING Chang-Ling<sup>1</sup> YOU Zhong-Lu<sup>\*1</sup>

(<sup>1</sup>Department of Chemistry and Chemical Engineering, Liaoning Normal University, Dalian, Liaoning 116029, China)

(<sup>2</sup>Liaoxi Yuming High School, Jinzhou, Liaoning 121000, China)

**Abstract:** A bis-Schiff base *N,N'*-bis(3,5-difluorosalicylidene)-1,3-diaminopropane ( $H_2L$ ) was prepared. Reaction of  $H_2L$  and manganese acetate with ammonium thiocyanate or sodium azide in methanol gave complexes  $[MnL(NCS)(OH_2)]$  (**1**) and  $[MnL(\mu_{1,3}-N_3)]_n$  (**2**), respectively.  $H_2L$  and the complexes were characterized by elemental analysis, IR spectra, <sup>1</sup>H NMR spectra, and the crystal structures of the complexes were analyzed by single crystal X-ray diffraction. The Schiff base ligand coordinates to the Mn atom through the imino nitrogen and phenolate oxygen. The thiocyanate ligand coordinates to the Mn atom through the nitrogen atom, and the azide ligand coordinates to the Mn atom, with a bridging mode, through two terminal nitrogen atoms. In both complexes, the Mn atoms adopt octahedral coordination. The Schiff base and the complexes were tested for their Jack bean urease inhibitory activities. For complex **1**, the inhibition rate at concentration of  $100 \mu\text{mol}\cdot\text{L}^{-1}$  on the urease is  $(52.0\pm 3.1)\%$ , and the  $IC_{50}$  value is  $(81.0\pm 3.7) \mu\text{mol}\cdot\text{L}^{-1}$ . While for complex **2**, it has no activity against the urease. Molecular docking study of complex **1** was performed to study the inhibition. CCDC: 1817812, **1**; 1817813, **2**.

**Keywords:** Schiff base; manganese(III) complex; crystal structure; urease inhibitor

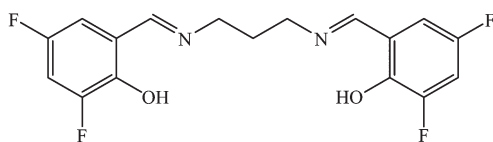
收稿日期: 2018-01-20。收修改稿日期: 2018-03-15。

国家自然科学基金(No.21641012)、辽宁省教育厅基金(No.LF201783611)和辽宁省大学生创新创业基金(No.201610165068)资助项目。

\*通信联系人。E-mail: youzhonglu@126.com; 会员登记号: S06N0019M1605。

## 0 Introduction

Urease (EC 3.5.1.5; urea amidohydrolase) is a binuclear nickel-dependent hydrolase enzyme, which can be synthesized by numerous organisms, including plants, bacteria, algae, fungi, and invertebrates, and occurs widely in animal and soil<sup>[1-2]</sup>. Urease enzyme catalyzes the decomposition of urea into ammonia and carbon dioxide in high efficiency<sup>[3]</sup>, with the rate of catalyzed reaction  $10^{14}$  times higher than the non-catalyzed reaction<sup>[4]</sup>. The enzyme possesses harmful effects on both human health and fertile soil. Bacterial urease is a virulent factor including the formation of infection stones, pyelonephritis, peptic ulceration, hepatic encephalopathy, and other diseases<sup>[5-6]</sup>. High urease activity in soil leads to increase ammonia toxicity in air and economic problems<sup>[7-8]</sup>. All these negative effects oblige us to explore effective urease inhibitors. And, in fact, urease inhibitors are now considered as the first line of treatment for infections caused by urease-producing microorganisms. Our research group has pioneered the study of Schiff base and their complexes as urease inhibitors<sup>[9-13]</sup>. Although, a variety of urease inhibitors have been investigated in the past, such as quinolones<sup>[14]</sup>, phosphoric triamides<sup>[15]</sup>, and thioureas<sup>[16]</sup>. Most of these compounds are banned from using *in vivo* because of their toxicity, instability, or severe side effects. So, it is crucial to synthesize new potent urease inhibitors with good stability, bioavailability, and low toxicity. Schiff bases have been reported as effective antibacterial agents<sup>[17-18]</sup>, and show interesting urease inhibitory activity<sup>[19]</sup>. Metal complexes have been proved to possess significant inhibitory activities on various enzymes<sup>[20-21]</sup>. As a part of our ongoing research on urease inhibition with metal complexes, two manganese(III) complexes were prepared and screened for their urease inhibition activity. The mechanism of urease inhibition was studied by using docking techniques.



Scheme 1 Structure of the Schiff base  $H_2L$

## 1 Experimental

### 1.1 General methods and materials

Starting materials, reagents and solvents were purchased from commercial suppliers with AR grade, and used without purification. Elemental analyses were performed on a Perkin-Elmer 240C elemental analyzer. IR spectra were recorded on a Jasco FT/IR-4000 spectrometer as KBr pellets in the  $4\,000\sim200\text{ cm}^{-1}$  region.  $^1\text{H}$  NMR spectrum for  $H_2L$  was recorded on a Bruker spectrometer at 500 MHz. X-ray diffraction was carried out on a Bruker SMART 1000 CCD diffractometer.

### 1.2 Synthesis of $H_2L$

3,5-Difluorosalicylaldehyde (3.16 g, 0.02 mol) and propane-1,3-diamine (0.74 g, 0.01 mol) were reacted in 50 mL methanol. The mixture was stirred at room temperature for 30 min to give a clear yellow solution. The solution was evaporated by distillation to give yellow solid product, which was recrystallized from ethanol to give  $H_2L$ . Yield 87%. Anal. Calcd. for  $C_{17}H_{14}F_4N_2O_2$ (%): C, 57.6; H, 4.0; N, 7.9. Found(%): C, 57.4; H, 3.9; N, 8.0. IR data ( $\text{cm}^{-1}$ ): 1 637 (s, C=N), 1 487 (s), 1 402 (w), 1 266 (m), 1 123 (w).  $^1\text{H}$  NMR (500 MHz,  $\text{CDCl}_3$ ):  $\delta$  13.45 (s, 2H, OH), 8.35 (s, 2H, CH=N), 6.96 (s, 2H, ArH), 6.80 (s, 2H, ArH), 3.78 (t, 4H,  $\text{CH}_2$ ), 2.18 (m, 2H,  $\text{CH}_2$ ).

### 1.3 Syntheses of complexes **1** and **2**

A methanolic solution (30 mL) of manganese acetate tetrahydrate (0.25 g, 1.0 mmol) was added to a methanolic solution (30 mL) of  $H_2L$  (0.35 g, 1.0 mmol) and ammonium thiocyanate (0.076 g, 1.0 mmol) for **1** or sodium azide (0.065 g, 1.0 mmol) for **2** with stirring. The mixture was stirred at room temperature for 30 min to give a brown solution. The resulting solution was allowed to stand in air for a few days until three quarter of the solvent was evaporated. Brown block-shaped crystals of the complex, suitable for X-ray single crystal diffraction were formed at the bottom of the vessel. The crystals were isolated by filtration, washed three times with cold methanol and dried in air.

Complex **1**: Yield: 37%. Anal. Calcd. for  $C_{18}H_{14}F_4MnN_3O_5S$ (%): C, 44.7; H, 2.9; N, 8.7. Found(%): C,

44.9; H, 3.0; N, 8.6. IR data ( $\text{cm}^{-1}$ ): 2 054 (s, NCS), 1 615 (s, C=N), 1 564 (m), 1 458 (s), 1 348 (m), 1 295 (m), 1 273 (m), 1 127 (m), 995 (w), 828 (m), 645 (w), 550 (w), 440 (w).

Complex **2**: Yield: 45%. Anal. Calcd. for  $\text{C}_{17}\text{H}_{12}\text{F}_4\text{MnN}_3\text{O}_2$ (%): C, 45.5; H, 2.7; N, 15.6. Found(%): C, 45.4; H, 2.7; N, 15.8. IR data ( $\text{cm}^{-1}$ ): 2 035 (s,  $\text{N}_3$ ), 1 615 (s, C=N), 1 564 (m), 1 463 (s), 1 355 (m), 1 292 (m), 1 267 (m), 1 131 (m), 1 058 (w), 995 (w), 828 (s), 746 (w), 640 (w), 540 (w), 435 (w).

#### 1.4 X-ray crystallography

Diffraction intensities for the complexes were collected at 298(2) K using a Bruker SMART 1000 CCD area-detector diffractometer with Mo  $K\alpha$  radiation ( $\lambda=0.071\ 073\ \text{nm}$ ). The collected data were reduced

with SAINT<sup>[22]</sup>, and multi-scan absorption correction was performed using SADABS<sup>[23]</sup>. Structures of the complexes were solved by direct methods and refined against  $F^2$  by full-matrix least-squares method using SHELXTL<sup>[24]</sup>. All of the non-hydrogen atoms were refined anisotropically. The hydrogen atoms attached to water ligand of complex **1** were located from a difference Fourier map and refined isotropically, with O-H and H $\cdots$ H distances restrained to 0.085(1) and 0.137(2) nm, respectively. The remaining hydrogen atoms were placed in calculated positions and constrained to ride on their parent atoms. Crystallographic data for the complexes are summarized in Table 1. Selected bond lengths and angles are given in Table 2.

CCDC: 1817812, **1**; 1817813, **2**.

Table 1 Crystallographic and refinement parameters for the complexes

	1	2
Formula	$\text{C}_{18}\text{H}_{14}\text{F}_4\text{MnN}_3\text{O}_3\text{S}$	$\text{C}_{17}\text{H}_{12}\text{F}_4\text{MnN}_3\text{O}_2$
Formula weight	483.3	449.3
Crystal system	Monoclinic	Orthorhombic
Space group	$P2_1/n$	$Pna2_1$
$a / \text{nm}$	1.291 9(5)	1.170 2(1)
$b / \text{nm}$	0.724 92(3)	1.293 1(2)
$c / \text{nm}$	2.033 3(1)	1.101 0(2)
$\beta / (^\circ)$	94.858(2)	
$V / \text{nm}^3$	1.897 4(2)	1.665 9(4)
$Z$	4	4
$D_c / (\text{g}\cdot\text{cm}^{-3})$	1.692	1.791
$\mu(\text{Mo } K\alpha) / \text{mm}^{-1}$	7.299	0.862
$F(000)$	976	904
Independent reflection	3 368	3 031
Observed reflection [ $I \geq 2\sigma(I)$ ]	2 787	2 407
Parameter	277	262
Restraint	3	1
Final $R$ indices [ $I \geq 2\sigma(I)$ ]	$R_1=0.067\ 0$ , $wR_2=0.179\ 7$	$R_1=0.038\ 4$ , $wR_2=0.078\ 9$
$R$ indices (all data)	$R_1=0.077\ 0$ , $wR_2=0.196\ 8$	$R_1=0.051\ 5$ , $wR_2=0.083\ 8$
GOF on $F^2$	1.045	0.939

Table 2 Selected bond lengths (nm) and angles ( $^\circ$ ) for the complexes

1					
Mn1-O1	0.190 0(3)	Mn1-O2	0.189 2(3)	Mn1-N1	0.205(4)
Mn1-N2	0.204 0(4)	Mn1-N3	0.218 8(4)	Mn1-O3	0.228 6(3)
O2-Mn1-O1	89.79(13)	O2-Mn1-N1	178.82(15)	O1-Mn1-N1	91.28(14)
O2-Mn1-N2	88.88(14)	O1-Mn1-N2	170.07(14)	N1-Mn1-N2	89.98(15)

Continued Table 2

O2-Mn1-N3	91.12(16)	O1-Mn1-N3	98.12(16)	N1-Mn1-N3	89.20(17)
N2-Mn1-N3	91.75(16)	O2-Mn1-O3	90.53(13)	O1-Mn1-O3	86.65(13)
N1-Mn1-O3	89.06(13)	N2-Mn1-O3	83.52(13)	N3-Mn1-O3	174.96(15)
2					
Mn1-O1	0.187 4(3)	Mn1-O2	0.187 4(3)	Mn1-N1	0.205 8(3)
Mn1-N2	0.202 0(3)	Mn1-N3	0.228 5(3)	Mn1-N5A	0.235 1(4)
O2-Mn1-O1	85.01(11)	O2-Mn1-N2	89.07(11)	O1-Mn1-N2	172.59(12)
O2-Mn1-N1	174.75(13)	O1-Mn1-N1	90.94(12)	N2-Mn1-N1	95.22(13)
O2-Mn1-N3	93.62(13)	O1-Mn1-N3	94.70(13)	N2-Mn1-N3	90.10(12)
N1-Mn1-N3	83.37(12)	O2-Mn1-N5A	102.34(12)	O1-Mn1-N5A	88.04(13)
N2-Mn1-N5A	88.89(13)	N1-Mn1-N5A	80.81(12)	N3-Mn1-N5A	163.99(13)

### 1.5 Urease inhibitory activity assay

The measurement of urease inhibitory activity was carried out according to the literature method<sup>[25]</sup>. The assay mixture containing 75  $\mu\text{L}$  of Jack bean urease and 75  $\mu\text{L}$  of tested compounds with various concentrations (dissolved in DMSO) was pre-incubated for 15 min on a 96-well assay plate. Acetohydroxamic acid was used as a reference. Then 75  $\mu\text{L}$  of phosphate buffer at pH 6.8 containing phenol red ( $0.18 \text{ mmol} \cdot \text{L}^{-1}$ ) and urea ( $400 \text{ mmol} \cdot \text{L}^{-1}$ ) were added and incubated at room temperature. The reaction time required for enough ammonium carbonate to form to raise the pH value of phosphate buffer from 6.8 to 7.7 was measured by micro-plate reader (560 nm) with end-point being determined by the color change of phenol-red indicator.

### 1.6 Molecular docking study

Molecular docking study of the complexes into the 3D X-ray structure of the Jack bean urease (entry 4UBP in the Protein Data Bank) was carried out by using the AutoDock 4.0 software as implemented through the graphical user interface AutoDockTools (ADT 1.5.2). The graphical user interface Auto Dock Tools was employed to setup the enzymes: all hydrogens were added, Gasteiger charges were calculated and nonpolar hydrogens were merged to carbon atoms. The Ni initial parameters are set as  $r=0.117 0 \text{ nm}$ ,  $q=+2.0$ , and van der Waals well depth of  $0.419 \text{ kJ} \cdot \text{mol}^{-1}$ <sup>[26]</sup>. The 3D structure of the ligand molecule was saved in pdb format with the aid of the program Mercury. The

resulting files were saved as pdbqt format.

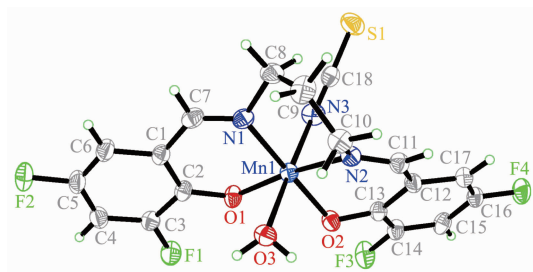
The AutoDockTools was used to generate the docking input files. In the docking, grid box size of  $70 \times 60 \times 60$  for complex **1** points in  $x$ ,  $y$ , and  $z$  directions was built, the maps were centered on the original ligand molecule (HAE) in the catalytic site of the protein. A grid spacing of  $0.037 5 \text{ nm}$  and a distances-dependent function of the dielectric constant were used for the calculation of the energetic map. 100 runs were generated by using Lamarckian genetic algorithm searches. Default settings were used with an initial population of 50 randomly placed individuals, a maximum number of  $2.5 \times 10^6$  energy evaluations, and a maximum number of  $2.7 \times 10^4$  generations. A mutation rate of 0.02 and a crossover rate of 0.8 were chosen. The results of the most favorable free energy of binding were selected as the resultant complex structures.

## 2 Results and discussion

### 2.1 Structure description of complex 1

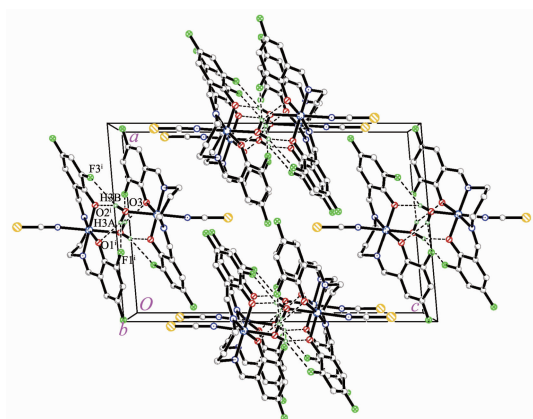
Molecular structure of complex **1** is shown in Fig. 1. The Schiff base ligand coordinates to the Mn atom through the phenolate O and imino N atoms. The Mn atom is in an octahedral coordination, with the four donor atoms of the Schiff base ligand defining the equatorial plane, and with the water O atom and thiocyanate N atom occupying the axial positions. The coordination bond lengths in the complex are comparable to those observed in manganese(III) complexes with Schiff base ligands<sup>[27-28]</sup>. The displacement of the

Mn atom from the equatorial plane towards the axial thiocyanate ligand is 0.008 8(2) nm. The dihedral angle between the two benzene rings of the Schiff base ligand is 19.2(5)°. In the crystal structure of the complex, molecules are linked through intermolecular O–H···O and O–H···F hydrogen bonds to form dimers (Fig.2).



Thermal ellipsoids are drawn at 30% probability level

Fig.1 Perspective view of the molecular structure of **1** with the atom labeling scheme



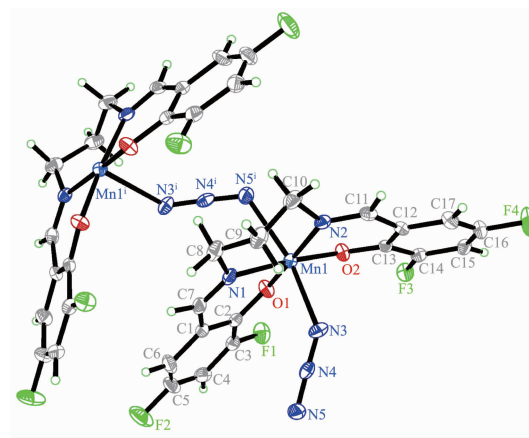
Hydrogen bonds are shown as dashed lines; Symmetry codes:  $i$  1-x, 1-y, -z

Fig.2 Molecular packing diagram of **1**

## 2.2 Structure description of complex 2

Molecular structure of complex **2** is shown in Fig. 3. The complex is an end-to-end azido-bridged polymeric manganese(III) compound. The Schiff base ligand coordinates to the Mn atom through the phenolate O and imino N atoms. The Mn atom is in an octahedral

coordination, with the four donor atoms of the Schiff base ligand defining the equatorial plane, and with two azido N atoms occupying the axial positions. The coordination bond lengths in the complex are similar to complex **1**, and also comparable to those observed in manganese(III) complexes with Schiff base ligands<sup>[27-28]</sup>. The displacement of the Mn atom from the equatorial plane is 0.000 9(2) nm. The dihedral angle between the two benzene rings of the Schiff base ligand is 35.5(4)°. In the crystal structure of the complex, molecules are linked through end-to-end azido ligands, to form 1D chains along *c*-axis direction (Fig.4).



Thermal ellipsoids are drawn at 30% probability level; Symmetry codes:  $i$  1-x, 1-y, -z

Fig.3 Perspective view of the molecular structure of **2** with the atom labeling scheme

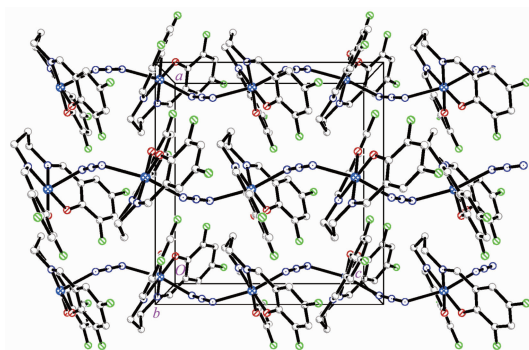


Fig.4 Molecular packing diagram of **2**

Table 3 Hydrogen bond parameters for complex **1**

D–H···A	<i>d</i> (D–H) / nm	<i>d</i> (H···A) / nm	<i>d</i> (D···A) / nm	∠D–H···A / (°)
O3–H3B···O2 <sup>i</sup>	0.085(1)	0.201(4)	0.277 9(4)	149(6)
O3–H3B···F3 <sup>i</sup>	0.085(1)	0.254(5)	0.235(4)	140(6)
O3–H3A···F1 <sup>i</sup>	0.085(1)	0.214(2)	0.944(5)	156(5)
O3–H3A···O1 <sup>i</sup>	0.085(1)	0.237(5)	0.291 9(4)	123(5)

Symmetry code:  $i$  1-x, 1-y, -z.



## 2.2 IR spectra

The weak and broad absorptions in the range of 3 300~3 500  $\text{cm}^{-1}$  in the spectra of  $\text{H}_2\text{L}$  and complex **1** substantiate the presence of O-H groups, which are absent in complex **2**. The strong absorption band at 1 637  $\text{cm}^{-1}$  for  $\text{H}_2\text{L}$  is assigned to the azomethine  $\nu(\text{C}=\text{N})$ , which is shifted to lower wavenumber in the spectra of the complexes, 1 615  $\text{cm}^{-1}$ . This indicates the coordination through the two imino N atoms. The typical intense absorptions at 2 054  $\text{cm}^{-1}$  for complex **1** and 2 035  $\text{cm}^{-1}$  for complex **2** are assigned to the

thiocyanate and azide groups, respectively.

## 2.3 Pharmacology

Results of the urease inhibition are summarized in Table 4. Acetohydroxamic acid and manganese acetate were used as references. The free Schiff base and complex **2** showed poor inhibition, while complex **1** showed effective inhibition, with  $\text{IC}_{50}$  value of  $(81.0 \pm 3.7) \mu\text{mol} \cdot \text{L}^{-1}$ . The urease inhibition of the manganese complex is weaker than Schiff base copper(II) complexes, but higher than Schiff base zinc(II) complexes reported previously<sup>[10,13,29-30]</sup>.

Table 4 Inhibition of urease by the tested materials

Tested material	Inhibition rate / %	$\text{IC}_{50} / (\mu\text{mol} \cdot \text{L}^{-1})$
$\text{H}_2\text{L}$	$12.3 \pm 2.0$	—
Complex <b>1</b>	$52.0 \pm 3.1$	$81.0 \pm 3.7$
Complex <b>2</b>	$31.6 \pm 2.5$	—
Manganese acetate	$18.7 \pm 1.2$	—
Acetohydroxamic acid	$87.5 \pm 4.0$	$39.8 \pm 3.4$

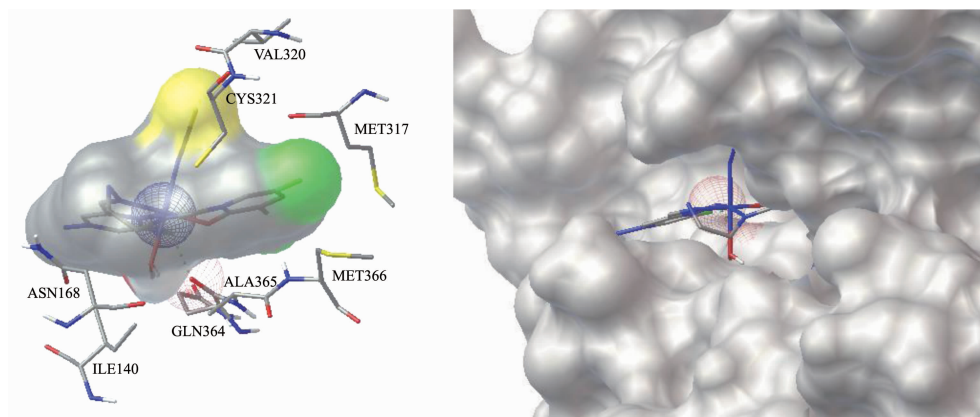
<sup>a</sup> Concentration of the tested material is 100  $\mu\text{mol} \cdot \text{L}^{-1}$ .

## 2.4 Molecular docking study

Molecular docking study was performed to investigate the binding effects between the molecule of complex **1** and the active site of the Jack bean urease. The binding model is depicted in Fig.5. The results revealed that the molecule of complex **1** fit well with the active pocket of the urease. Additional interactions have been established in a variety of conformations because of the flexibility of the complex molecule and the amino acid residues of the enzyme.

The optimized clusters (100 occurrences each) were ranked by energy level in the best conformation of inhibitor-urease modeled structures, where the docking score is -6.24. The negative value indicates that the molecule bind well with the urease. As a comparison, the docking score for the AHA inhibited model is -5.01.

The mechanism of urease inhibition was considered to be blockage of the entrance of the urease active pocket and the interaction of residues.



Left: Only the interacting residues are displayed and the interactions are shown as dashed spheres;

Right: Enzyme is shown as surface and the complex is shown as sticks

Fig.5 Binding mode of complex **1** with the urease

The results endorse that complex **1** may serve as a structural template for the design and development of novel urease inhibitors.

### 3 Conclusions

The present study reports syntheses, characterization and crystal structures of two Schiff base manganese(III) complexes with bis-Schiff bases. The Schiff base ligand coordinates to the Mn atoms through the phenolate oxygen and imino nitrogen. The other sites of the octahedral coordination are occupied by water, thiocyanate or azide ligands. The thiocyanato-coordinated mononuclear complex has effective inhibitory activity against Jack bean urease, while the azido-bridged polymeric complex has no activity. Considering that Schiff base manganese complexes have interesting biological activities, complex **1** described here may be used as a precursor for the design of novel urease inhibitors.

### References:

- [1] Myrach T, Zhu A T, Witte C P. *J. Biol. Chem.*, **2017**,**292**: 14556-14565
- [2] Arshad T, Khan K M, Rasool N, et al. *Bioorg. Chem.*, **2017**, **72**:21-31
- [3] Mira A B, Cantarella H, Souza-Netto G J M, et al. *Agric. Ecosyst. Environ.*, **2017**,**248**:105-112
- [4] Dempsey R J, Slaton N A, Norman R J, et al. *Agron. J.*, **2017**,**109**:363-377
- [5] Taha M, Ismail N H, Imran S, et al. *J. Bioorg. Med. Chem.*, **2015**,**23**:7211-7218
- [6] Amtul Z, Siddiqui R A, Choudhary M I. *Curr. Med. Chem.*, **2002**,**9**:1323-1348
- [7] Aslam M A S, Mahmood S U, Shahid M, et al. *Eur. J. Med. Chem.*, **2011**,**46**:5473-5479
- [8] Saeed A, Khan M S, Rafique H. *Bioorg. Chem.*, **2014**,**52**:1-7
- [9] Jing C L, Wang C F, Yan K, et al. *Bioorg. Med. Chem.*, **2016**, **24**:270-276
- [10] You Z L, Liu M Y, Wang C F, et al. *RSC Adv.*, **2016**,**6**: 16679-16690
- [11] Qu D, Niu F, Zhao X L, et al. *Bioorg. Med. Chem.*, **2015**, **23**:1944-1949
- [12] You Z L, Yu H Y, Zheng B Y, et al. *Inorg. Chim. Acta*, **2018**,**469**:44-50
- [13] Pan L, Wang C F, Yan K, et al. *J. Inorg. Biochem.*, **2016**, **159**:22-28
- [14] Abdullah M A A, Abuo-Rahma G E A A, Abdelhafez E M N, et al. *Bioorg. Chem.*, **2017**,**70**:1-11
- [15] Mazzei L, Cianci M, Contaldo U, et al. *Biochemistry*, **2017**, **56**:5391-5404
- [16] Saeed A, Ur-Rehman S, Channar P A, et al. *Drug Res.*, **2017**,**67**:596-605
- [17] XIE Qing-Fan(解庆范), GUO Miao-Li(郭妙莉), CHEN Yan-Min(陈延民). *Chinese J. Inorg. Chem.*(无机化学学报), **2018**,**34**:309-316
- [18] SHI Juan(史娟), LI Jiang(李江), GE Hong-Guang(葛红光). *Chinese J. Inorg. Chem.*(无机化学学报), **2017**,**33**:463-470
- [19] Khan K M, Rahim F, Khan A, et al. *J. Chem. Soc. Pak.*, **2015**,**37**:479-483
- [20] Qin Q P, Meng T, Tan M X, et al. *Eur. J. Med. Chem.*, **2018**, **143**:1597-1603
- [21] Oliveri V, Lanza V, Milardi D, et al. *Mettallomics*, **2017**,**9**: 1439-1446
- [22] SMART Ver. 5.628 and SAINT Ver. 6.02, Bruker AXS, Madison, Wisconsin, USA, **1998**.
- [23] Sheldrick G M. *SADABS, Program for Empirical Absorption Correction of Area Detector*, University of Göttingen, Germany, **1996**.
- [24] Sheldrick G M. *Acta Crystallogr. Sect. A: Found. Crystallogr.*, **2008**,**A64**:112-122
- [25] Mao W J, Lv P C, Shi L, et al. *Bioorg. Med. Chem.*, **2009**, **17**:7531-7536
- [26] Krajewska B, Zaborska W. *Bioorg. Chem.*, **2007**,**35**:355-365
- [27] You Z L, Liu T, Zhang N, et al. *Inorg. Chem. Commun.*, **2012**,**19**:47-50
- [28] Zhang N, Huang C Y, Shi D H, et al. *Inorg. Chem. Commun.*, **2011**,**14**:1636-1639
- [29] Wang J, Qu D, Lei J X, et al. *J. Coord. Chem.*, **2017**,**70**: 544-555
- [30] Lu Y, Shi D H, You Z L, et al. *J. Coord. Chem.*, **2012**,**65**: 339-352